Research Article

Olivier Parriaux* and Yves Jourlin

Design of a 1D phase-mask translational scanner for large-size spatially coherent grating printing

https://doi.org/10.1515/aot-2018-0017
Received March 20, 2018; accepted May 16, 2018; previously published online June 12, 2018

Abstract: Controlled translational displacement between a large-surface photosensitive planar substrate and a wide and short 1D grating phase-mask enables the printing of large-width, spatially highly coherent gratings of principally unlimited length, using a limited number of opto-mechanical control parameters. The phase-mask is illuminated by a temporally modulated exposure light sheet controlled by a displacement sensor. The proposed method is compared with existing techniques, and its functional elements and their combination are analyzed.

Keywords: diffraction and gratings; optical engineering; optical fabrication; photolithography.

OCIS codes: 050.0050; 110.5220; 120.4610; 350.4600.

1 Introduction

Printing large-area optical gratings with high spatial coherence has been of interest since the invention of the chirped pulse amplification (CPA) scheme [1], whereby a temporally stretched optical pulse is first amplified and, then, is temporally compressed down to a few tens of femtoseconds using a pair of diffraction gratings. In applications such as controlled thermonuclear fusion [2], the fluence is so large, and the optical damage threshold of the best dielectric multilayers [3] is so limited that ensuring a supra-threshold state is only possible by increasing the grating area. However, increasing the area of high spatial coherence gratings is faced with practical difficulties: all processes, including the handling, photoresist processing, and corrugation etching of large substrates, require specific large-size equipment, whereas ensuring wide beams in the single-shot interferogram exposure scheme [4] requires large optical elements such as parabolic mirrors, increasing the demand for the mechanical and optical path stability. This leads to investment and running costs that increase supra-linearly with increasing grating area. This explains the preference for resorting to side-by-side tiling using two or more standard-size gratings, typically with a 1-m^2 area [5]. Such a scheme is not without difficulty either because ensuring coplanarity, grating line parallelism, and period phase matching within a fraction of a period increases the complexity of the pulse compression subsystem.

An alternative large-grating printing strategy was proposed [6] and developed [7], whereby a small elementary interferogram spot is scanned over the photoresist-coated substrate area. This approach reduces the problem of the large-beam conditioning to that of controlling the scan of two narrow overlapping and interfering beams and can also be used to define a uniform, single spatial frequency grating composed of strictly straight and parallel lines without phase jumps. This fabrication strategy is highly flexible and, in principle, allows printing large gratings with a spatially dependent distribution of spatial frequency. Another printing strategy was proposed and demonstrated recently [8], which consists of a broad-beam scanning exposure using a latent grating continuously generated during scanning for real-time dynamic fringe locking. This approach can potentially yield unlimited recording length.

The printing strategy described here also aims at the definition of a wide single spatial frequency grating of unlimited length, but it does so by combining the scan of a subset of the grating with the diffraction of a thin and wide incident sheet of light by means of a short and wide phase-mask. This combination of the laterally uniform and temporally modulated illumination of the grating subset and of its one-dimensional (1D) scan results from an insightful allocation of the grating's spatial coherence characteristics. The fabrication of the wide phase-mask can be made using a small phase-mask, mechanically scanned, this

***Corresponding author: Olivier Parriaux,** Univ Lyon, UJM-Saint-Etienne, CNRS, Institut d'Optique Graduate School, Laboratoire Hubert Curien UMR 5516, F-42023 Saint-Etienne, France, e-mail: parriaux@univ-st-etienne.fr
Yves Jourlin: Univ Lyon, UJM-Saint-Etienne, CNRS, Institut d'Optique Graduate School, Laboratoire Hubert Curien UMR 5516, F-42023 Saint-Etienne, France

© 2018 THOSS Media and De Gruyter

time in the direction of the lines, and without exposure modulation. This leads to a rather simple optomechanical system implementation.

2 The printing strategy

A spatially highly coherent single spatial frequency grating is characterized by perfectly straight and parallel lines along the Y direction, positioned strictly periodically along the X direction normal to the lines, as schematically shown in Figure 1. Figure 1 shows the proposed continuous printing process of a wide grating with unlimited length along the X direction on a high rectilinearity translation bench. Manifestly, the elementary generic subset that can be photorepeated is a long, perfectly straight line. A single line can, however, not be projected and repeated along the X direction when the grating period is of the order or smaller than the printing wavelength, which is the case for an optical pulse compression stage [4]. Under this condition, the photorepeating of a straight line can only be achieved by making it a part of a set of identical, parallel and periodically distributed straight lines; in other words, the line is a part of the group of lines of a grating phase-mask [9]. This prerequisite turns out to be an advantage because a phase-mask projects its straight, parallel, periodic line pattern onto a resist-coated surface placed underneath; thus, the grating subset to be scanned along the X direction becomes a set of straight lines with its own spatial coherence characteristics on-board the phase-mask instead of a single straight line.

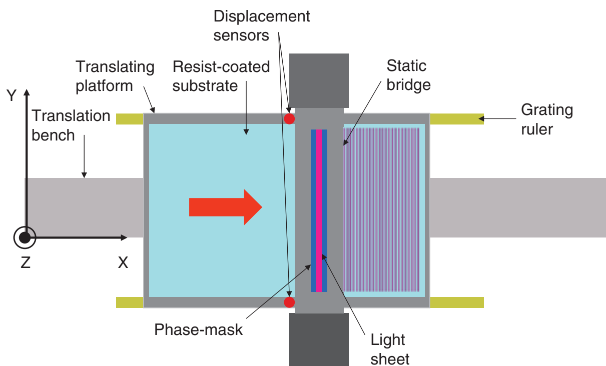

Figure 1: Schematic top view of the large grating fabrication method using the 1D scan along X of a wide photoresist-coated substrate under a long phase-mask suspended in a static bridge and illuminated by a temporally modulated light sheet.

The projected period is half that of the phase-mask if the light sheet is normally incident along the coordinate Z normal to the XY plane (Figure 2A) and equal to that of the phase-mask if the incidence is under the –first-order Littrow condition, as shown schematically in Figure 2B. The set of dim and bright lines of the interferogram indicates the location of the interferogram relative to the phase-mask grating.

For a phase-mask to generate a single spatial frequency high-contrast interferogram in the case of normal incidence, the zeroth transmitted order must be suppressed [9], and the phase-mask period Λ must be between λ and 2λ (λ is the exposure wavelength in air), to enable the excitation of the two first orders and prevent the excitation of the second diffraction orders. The condition is simply $3\lambda/2>\Lambda>\lambda/2$ in the case of the –first-order Littrow incidence onto the phase-mask.

Thus, using a phase-mask of perfectly straight lines with the length adapted to the width of the large grating

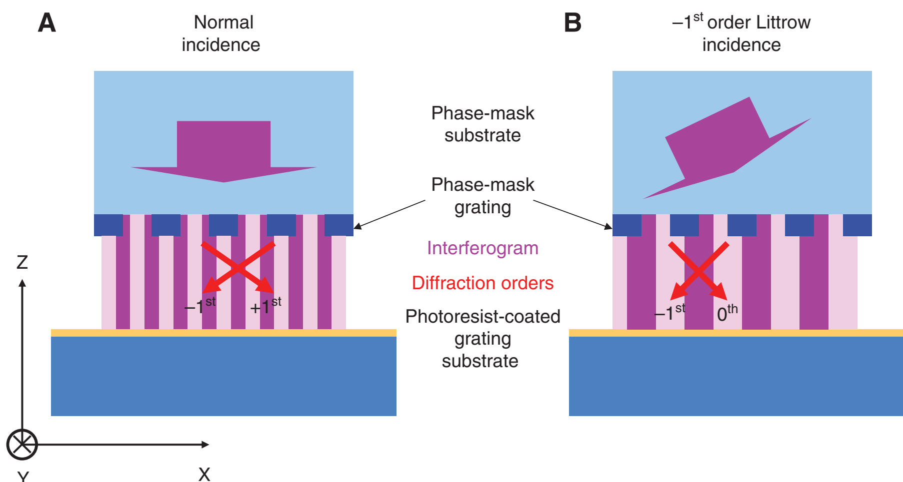

Figure 2: Cross-sectional view in Figure 1 normal plane of the generation of a periodic interferogram along the axis X using a phase-mask (A) for normal and (B) –first-order Littrow incidence, also showing the diffraction orders involved.

yields a set of perfectly straight lines on the resist-coated substrate. Moreover, if the phase-mask lines are perfectly parallel and periodic, the spatial coherence is achieved locally on the grating substrate. There is a very important advantage brought by the phase-mask: the projected period is independent of the spectral width (or temporal coherence) of the printing light sheet as well as of its angular width within the incident plane defined as normal to the grating lines. The only requirements – which are actually weak requirements – are on the polarization [the phase-mask corrugation is optimized for the transverse electric (TE) polarization to achieve the highest interference contrast] and on the width of the angular spectrum in the plane of incidence. The large tolerances on the spatial and temporal coherence of the mask transfer exposure beam can be compared with those prevailing for the two printing strategies cited above: a single-shot exposure [4] of a large-area grating requires both very high temporal and spatial coherence. The approach of the interference spot scanning [7] also requires high temporal coherence; it is less demanding as to the wave front, but it suffers from the fact that the latter is not uniform, which necessitates overlapping exposures to deliver a uniform dose all over the length of the grating lines, i.e. to ensure a uniform line/space ratio.

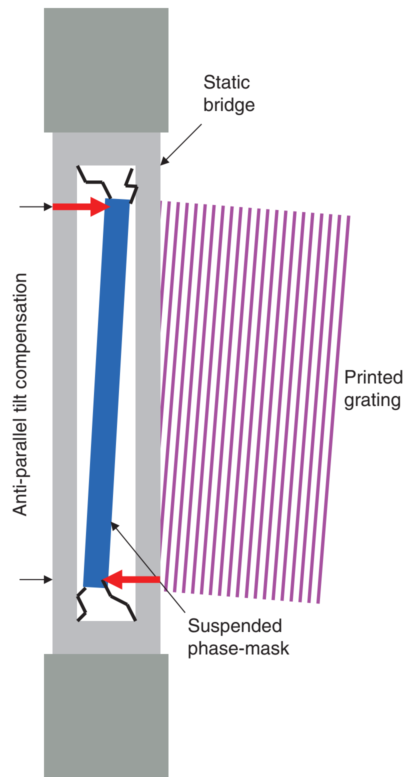

Figure 3: Top view in Figure 1 XY plane of the static bridge with suspended phase-mask. The yaw compensation principle ensures that the displacement difference measured by two displacement sensors is fed to two piezo-actuators that impose the correction phase-mask substrate tilt in the XY plane.

3 The scanning mode

With utmost straightness, parallelism, and periodicity being achieved holistically along the Y direction as embarked on-board the phase-mask, the scan along the X direction must strictly maintain the parallelism and periodicity upon its continuous translation along the X direction under the phase-mask. As to the parallelism, the critical parameter is the angular tilt in the XY plane of the substrate (or yaw). The tolerable tilt is below 0.1 μrad for a 1-m-wide grating and a slightly submicron-scale grating period. This can be achieved in two ways: The first is by using a very precisely ground translation bench [10]. Second, if the rectilinearity of the latter is not sufficient, the tilt can be controlled by means of two displacement sensors placed ~1 m from each other along the Y axis, which measure the displacement along the X direction. Any position difference measured by the sensors is fed back to a static bridge where the phase-mask is suspended in a monolithic frame made of elastic blades allowing to generate a real-time tilt owing to the anti-parallel action of two piezo-actuators. This yaw compensation scheme is illustrated in Figure 3.

At least one displacement sensor must be used because the exposure light sheet must be switched on and off during each period upon the translation, to ensure the desired periodicity. For displacement sensors consisting of interferometers [11], the refractive index of the air along the two light paths must be stabilized identically. An advantageous alternative approach consists of replacing the interferometers by two long-range high-resolution displacement sensors using Invar or Zerodur grating scales [12], as suggested in Figure 1.

As long as the yaw can be corrected, there is no limit on the length of the large printed grating, and the translation bench does not need to be of the highest precision and rectilinearity; the roll and pitch are not critical for ensuring high spatial coherence.

There is no particular requirement on the absolute position of the table in its continuous translation under the static bridge supporting the phase-mask. In order to avoid stitching problems between printed fields, the scanning steps – i.e. the exposure flashes – along the continuous table displacement X are synchronous with each period being printed. There is a feedback control between

the table displacement measurement sensors and the light source switching (or modulation) time intervals.

4 The phase-mask definition

The demands placed on the phase-mask spatial coherence are utmost straightness, parallelism, and identical spacing between the centers of consecutive lines and an identical line/space ratio. A quasi-perfect phase-mask could be printed using electron beam lithography. However, such an equipment cannot presently be used for printing structures on the length scale of 1 m [13]. An alternative approach is to scan a phase-mask along the grating lines without exposure beam switching, as we demonstrated experimentally earlier [14], and with an industrial laser printer [15]. The printing phase-mask is an e-beam written square grating spot illuminated by a TE-polarized collimated beam. The resist-coated long phase-mask substrate translates at a constant velocity on a long, precisely ground bench, ensuring rectilinearity better than 100 nm and lateral offset noise well under 100 nm as checked metrologically [10]. Figure 4 illustrates the longitudinal phase-mask scan for fabricating long grating phase-masks.

After the long phase-mask exposure, the photoresist corrugation is to be transferred into its hard substrate or high refractive index coating. Reactive ion (beam) etching (RI(B)E) has to be performed, preferably in a scanning mode, too [16]; the large-area technology is under development [17].

5 Exposure light sheet

The uniformity of the printed grating duty cycle depends on the uniformity of the light exposure dose along Y. There are several ways to obtain a polarized, switchable light sheet of uniform intensity along the Y direction, with restricted angular width in the plane of incidence. For instance, several solutions have been proposed and developed in the field of optical backplanes for display illumination. They usually comprise a thick waveguide in which the light of a source, placed at the edge, zig-zags and is diffracted out essentially normally by a variable-efficiency reflection grating or a set of microprism reflectors defined at one side of the waveguide [18]. Such widely used 2D optimized solutions can easily be simplified to 1D, for the generation of the desired light sheet. A preferred solution is, however, to take advantage of the temporal and angular coherence tolerances offered by a phase-mask approach and to generate an exposure light sheet next to the phase-mask in the form of a linear array of light-emitting diodes (LEDs) [19] or semiconductor lasers with their collimation optics [20] ensuring, as they do in their current application fields, a homogeneous distribution of the exposure dose along Y.

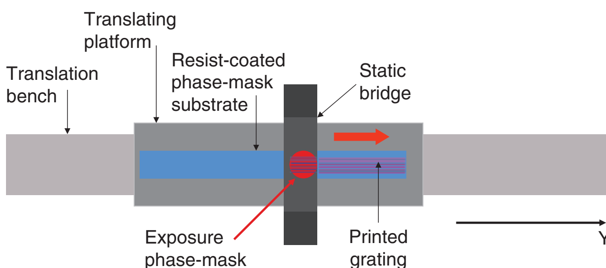

Figure 4: Long phase-mask fabrication by the continuous longitudinal scanning under the continuous wave exposure of a small phase-mask.

6 Method flexibility and application domains

As stated in Section 2, the range of phase-mask periods relative to the exposure wavelength for generating high-contrast interferograms is rather restricted. Referring to Figure 2 and related comments, printing small periods amounts to selecting the normal incidence scheme (Figure 1A) and decreasing the exposure wavelength λ. The smallest practicable wavelength for phase-mask exposure today is 193 nm emitted by ArF excimer lasers. This implies that the smallest printable period is slightly above 100 nm. To extend the range to smaller periods, it is possible to resort to immersion lithography, as we demonstrated for a printed period of 100 nm in Ref. [21]; with an ArF laser, slightly sub-100-nm periods are within reach. Extending the range to larger periods without the excitation of higher diffraction orders is possible using a dual-grating phase-mask that simulates a heterodyne scheme in the spatial frequency domain as we demonstrated in Ref. [22]. An important last step in a grating manufacturing process is the control of the spatial coherence. The test of the regularity of the period over the whole grating area can also be made in a scanning mode as described and demonstrated in Ref. [23], whereby a monolithic optical double read-head, flying over the grating under test with fixed spacing between both heads, achieves the interference between the orders diffracted by the grating. The variation of the

detected electrical phase difference between the two heads gives the variation of the grating period with a resolution better than 1 pm.

With regard to the application domains, the prime motivation for the development of the described concept is to offer a simpler and lower-cost fabrication technology of even larger gratings while preserving the needed specifications on the spatial coherence. This method could also be implemented for fabricating vacuum ultraviolet and soft X-ray gratings [24], as well as for phase-contrast X-ray imaging [25], where high spatial coherence is required. Further, owing to its simplicity, the method can be used for fabricating large-grating templates for low-end replication [26] in case an improvement of the spatial coherence is desired. Different fields of applications require different grating profiles: printing binary gratings as needed for pulse compression requires highly non-linear photoresists associated with exposure switching upon the phase-mask scan. It is also possible to fabricate sinusoidal as well as blazed corrugation profiles using a linear photoresist with the corresponding synchronous light sheet modulation at the period scale.

References

[1] D. Strickland and G. Mourou, Opt. Com. 56, 219–221 (1985).
[2] R. Betti and O. A. Hurricane, Nat. Phys. 12, 435–448 (2016).
[3] D. Alessi, C. W. Carr, R. A. Negres, R. P. Hackel, K. A. Stanion, et al., Proc. SPIE 9345, 934509 (2015).
[4] H. T. Nguyen, J. A. Britten, T. C. Carlson, J. D. Nissen, L. J. Summers, et al., Proc. SPIE 5991, 443–448 (2005).
[5] Y. Yang, X. Wang, J. Zhang, H. Luo, F. Li, et al., Opt. Lasers Eng. 50, 262–267 (2012).
[6] M. Schattenburg and P. N. Everett, US patent 6,882,477 B1 (2005).
[7] J. C. Montoya, C.-H. Chang, R. K. Heilmann and M. L. Schattenburg, J. Vac. Sci. Technol. B 23, 2640–2645 (2005).
[8] D. Ma, Y. Zhao and L. Zeng, Sci. Rep. 7, 926 (2017).
[9] E. Gamet, A. V. Tishchenko and O. Parriaux, Appl. Opt. 46, 6719–6726 (2007).
[10] www.kunz-precision.ch (Jan. 2018).
[11] www.renishaw.com/en/interferometric-laser-encoders–6404 (Jan. 2018).
[12] www.heidenhain.de (Jan. 2018).
[13] www.vistec-semi.com (Jan. 2018).
[14] P. Müller, Y. Jourlin, C. Veillas, G. Bernaud, Y. Bourgin, et al., Opt. Eng. 50, 038001–038001-9 (2011).
[15] V. Gate, G. Bernaud, C. Veillas, A. Cazier, F. Vocanson, et al., Opt. Eng. 52, 091712 (2013).
[16] B. Xu, S. D. Smith, D. J. Smith and D. Chargin, in: Proc. Society Vacuum Coaters 505/856-7188, 50th Annual Technical Conference (2007).
[17] http://www.iom-leipzig.de/ionenstrahlgestuetzte-technologien/ (Jan. 2018).
[18] R. Shechter, Y. Amitai and A. A. Friesem, Appl. Opt. 41, 1236–1240 (2002).
[19] W. Henry and C. Percival, Society for Information Display Symposium Digest, May 22–May 27 (2016).
[20] J. F. Seurin, G. Xu, V. Khalfin, A. Miglo, J. D. Wynn, et al., Proc. SPIE 7229, 722903 (2009).
[21] Y. Bourgin, Y. Jourlin, O. Parriaux, A. Talneau, S. Tonchev, et al., Opt. Express 18, 10557–10566 (2010).
[22] Y. Bourgin, I. Vartiainen, Y. Jourlin, M. Kuittinen, F. Celle, et al., J. Eur. Opt. Soc.-Rapid Publication 6, 11016s (2011).
[23] Y. Jourlin, A. V. Tishchenko, C. Pedri and O. Parriaux, J. Vac. Sci. Technol. B 21, 3136–3139 (2003).
[24] R. K. Heilmann, M. Ahn and M. L. Schattenburg, Proc. SPIE 7011, 701106 (2008).
[25] J. Meiser, M. Willner, T. Schröter, A. Hofmann, J. Rieger, et al., J. Xray Sci. Technol. 24, 379–388 (2016).
[26] C.-W. Liu, C.-H. Lee and S.-C. Lin, J. Soc. Inf. Disp. 20, 646–652 (2012).